AFCEC-CX-TY-TR-2013-0008

EFFECT OF SOIL MOISTURE ON CHLORINE DEPOSITION (POSTPRINT)

John D. Hearn and Christopher D. Hare
Airbase Technologies Division
Air Force Research Laboratory
139 Barnes Drive, Suite 2
Tyndall Air Force Base, FL 32403-5323

Jeffery A. Eichler
Universal Technology Corporation
1270 North Fairfield Road
Dayton, OH 45432

Michael V. Henley
Requirements and Acquisitions Division
Air Force Civil Engineer Center
139 Barnes Drive, Suite 1
Tyndall AFB, FL 32403-5323

.

AIR FORCE CIVIL ENGINEER CENTER
READINESS DIRECTORATE

■ **Requirements & Acquisition Division** ■ **United States Air Force** ■ **Tyndall Air Force Base, FL 32403-5323**

Report Documentation Page		*Form Approved* *OMB No. 0704-0188*

Public reporting burden for the collection of information is estimated to average 1 hour per response, including the time for reviewing instructions, searching existing data sources, gathering and maintaining the data needed, and completing and reviewing the collection of information. Send comments regarding this burden estimate or any other aspect of this collection of information, including suggestions for reducing this burden, to Washington Headquarters Services, Directorate for Information Operations and Reports, 1215 Jefferson Davis Highway, Suite 1204, Arlington VA 22202-4302. Respondents should be aware that notwithstanding any other provision of law, no person shall be subject to a penalty for failing to comply with a collection of information if it does not display a currently valid OMB control number.

1. REPORT DATE **08 JUL 2013**	2. REPORT TYPE		3. DATES COVERED
4. TITLE AND SUBTITLE **Effect of Soil Moisture on Chlorine Deposition (POSTPRINT)**			5a. CONTRACT NUMBER
			5b. GRANT NUMBER
			5c. PROGRAM ELEMENT NUMBER
6. AUTHOR(S)			5d. PROJECT NUMBER
			5e. TASK NUMBER
			5f. WORK UNIT NUMBER
7. PERFORMING ORGANIZATION NAME(S) AND ADDRESS(ES) **Universal Technology Corp,1279 N. Fairfield Road,Dayton ,OH,45432**			8. PERFORMING ORGANIZATION REPORT NUMBER
9. SPONSORING/MONITORING AGENCY NAME(S) AND ADDRESS(ES)			10. SPONSOR/MONITOR'S ACRONYM(S)
			11. SPONSOR/MONITOR'S REPORT NUMBER(S)

12. DISTRIBUTION/AVAILABILITY STATEMENT
Approved for public release; distribution unlimited.

13. SUPPLEMENTARY NOTES
The original document contains color images.

14. ABSTRACT

The effect of soil moisture on chlorine (Cl2) deposition was examined in laboratory chamber experiments at high Cl2 exposures by measuring the concentration of chloride (Cl -) in the soil columns. Soil mixtures with varying amounts of clay, sand, and organic matter and with moisture contents up to 20% (w/w) were exposed to Cl2. For low water content soils, additional water increased the reaction rate as evidenced by higher Cl - concentration at higher soil moisture content. Results also showed that the presence of water restricted transport of Cl2 into the soil columns and caused lower overall deposition of Cl2 in the top 0.48 cm layer of soil when water filled ≈ 60% or more of the void space in the column. Numerical solutions to partial differential equations of Fick's law of diffusion and a simple rate law for Cl2 reaction corroborated conclusions derived from the data. For the soil mixtures and conditions of these experiments, moisture content that filled 30 -50% of the available void space yielded the maximum amount of Cl2 deposition in the top 0.48 cm of soil.

15. SUBJECT TERMS

16. SECURITY CLASSIFICATION OF:			17. LIMITATION OF ABSTRACT	18. NUMBER OF PAGES **7**	19a. NAME OF RESPONSIBLE PERSON
a. REPORT **unclassified**	b. ABSTRACT **unclassified**	c. THIS PAGE **unclassified**			

REPORT DOCUMENTATION PAGE

1. REPORT DATE (DD-MM-YYYY)	2. REPORT TYPE	3. DATES COVERED (From - To)
08-JUL-2013	Journal Article - POSTPRINT	01-JAN-2012 -- 31-DEC-2012

4. TITLE AND SUBTITLE

Effect of Soil Moisture on Chlorine Deposition (POSTPRINT)

5a. CONTRACT NUMBER
FA4819-11-C-0003

5b. GRANT NUMBER

5c. PROGRAM ELEMENT NUMBER
0909999F

6. AUTHOR(S)
#Hearn, John D.; *Eichler, Jeffery A.; #Hare, Christopher D., ^Henley, Michael V.

5d. PROJECT NUMBER
GOVT

5e. TASK NUMBER
L0

5f. WORK UNIT NUMBER
X13SY002 X0E7 (QL102007)

7. PERFORMING ORGANIZATION NAME(S) AND ADDRESS(ES)

*Universal Technology Corp   #Air Force Research Laboratory
 1270 North Fairfield Road   Materials and Manufacturing Directorate
 Dayton, OH 45432   Airbase Technologies Division
                                              139 Barnes Drive, Suite 2, Tyndall AFB, FL

8. PERFORMING ORGANIZATION REPORT NUMBER

9. SPONSORING/MONITORING AGENCY NAME(S) AND ADDRESS(ES)

^Air Force Civil Engineer Center
Readiness Directorate
Requirements and Acquisition Division
139 Barnes Drive, Suite 1
Tyndall Air Force Base, FL 32403-5323

10. SPONSOR/MONITOR'S ACRONYM(S)
AFCEC/CXA

11. SPONSOR/MONITOR'S REPORT NUMBER(S)
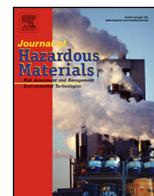AFCEC-CX-TY-TP-2013-0008

12. DISTRIBUTION/AVAILABILITY STATEMENT
DISTRIBUTION A. Approved for public release; distribution unlimited.
Available only to DTIC users. U.S. Government or Federal Purpose Rights License.

14. ABSTRACT

The effect of soil moisture on chlorine (Cl_2) deposition was examined in laboratory chamber experiments at high Cl_2 exposures by measuring the concentration of chloride (Cl^-) in the soil columns. Soil mixtures with varying amounts of clay, sand, and organic matter and with moisture contents up to 20% (w/w) were exposed to Cl_2. For low water content soils, additional water increased the reaction rate as evidenced by higher Cl^- concentration at higher soil moisture content. Results also showed that the presence of water restricted transport of Cl_2 into the soil columns and caused lower overall deposition of Cl_2 in the top 0.48 cm layer of soil when water filled $\approx$ 60% or more of the void space in the column. Numerical solutions to partial differential equations of Fick's law of diffusion and a simple rate law for Cl_2 reaction corroborated conclusions derived from the data. For the soil mixtures and conditions of these experiments, moisture content that filled 30 -50% of the available void space yielded the maximum amount of Cl_2 deposition in the top 0.48 cm of soil.

15. SUBJECT TERMS

hazard prediction, chlorine, toxic industrial chemical, deposition

16. SECURITY CLASSIFICATION OF:			17. LIMITATION OF ABSTRACT	18. NUMBER OF PAGES	19a. NAME OF RESPONSIBLE PERSON
a. REPORT	b. ABSTRACT	c. THIS PAGE	UU	7	Michael V. Henley
U	U	U			19b. TELEPHONE NUMBER (Include area code) 850 283 6050

Reset

Standard Form 298 (Rev. 8/98)
Prescribed by ANSI Std. Z39.18

CrossMark

Effect of soil moisture on chlorine deposition

John Hearn [a,*], Jeffery Eichler [b], Christopher Hare [a], Michael Henley [c]

[a] Air Force Research Laboratory, Airbase Technologies Division, 139 Barnes Dr. Suite 2, Tyndall AFB, FL 32403, United States
[b] Universal Technology Corporation, 139 Barnes Dr. Suite 2, Tyndall AFB, FL 32403, United States
[c] Air Force Civil Engineer Center, 139 Barnes Dr. Suite 2, Tyndall AFB, FL 32403, United States

HIGHLIGHTS

- Moisture increases chlorine's reaction rate with soil constituents.
- Moisture decreases chlorine's transport rate through the soil.
- Cl_2 deposition rate is maximized when water filled 30–50% of the soil void space.

ABSTRACT

The effect of soil moisture on chlorine (Cl_2) deposition was examined in laboratory chamber experiments at high Cl_2 exposures by measuring the concentration of chloride (Cl^-) in soil columns. Soil mixtures with varying amounts of clay, sand, and organic matter and with moisture contents up to 20% (w/w) were exposed to $\approx 3 \times 10^4$ ppm Cl_2 vapor. For low water content soils, additional water increased the reaction rate as evidenced by higher Cl^- concentration at higher soil moisture content. Results also showed that the presence of water restricted transport of Cl_2 into the soil columns and caused lower overall deposition of Cl_2 in the top 0.48-cm layer of soil when water filled $\approx 60\%$ or more of the void space in the column. Numerical solutions to partial differential equations of Fick's law of diffusion and a simple rate law for Cl_2 reaction corroborated conclusions derived from the data. For the soil mixtures and conditions of these experiments, moisture content that filled 30–50% of the available void space yielded the maximum amount of Cl_2 deposition in the top 0.48 cm of soil.

Published by Elsevier B.V.

1. Introduction

For toxic chemical releases, consequence assessment models must account for source terms, meteorology, dispersion rates, and chemical degradation (e.g., photolysis and deposition) to accurately predict a hazard zone. Chlorine (Cl_2) is a toxic industrial chemical that is of concern to the transportation and defense communities [1], but its fate is still not well characterized. Deposition has been mentioned as a potentially important factor in the fate of high-concentration Cl_2 plumes when model results are compared with observations from actual releases [2,3], and one modeling study focusing on dense gas deposition found that deposition may be important for some conditions but additional experimental investigations were needed [4]. Experimental measurements of Cl_2 uptake on aerosol particles [5,6], alfalfa grass [7], and soil [8] indicated that deposition is fast. In addition, measurements of Cl_2 deposition

during outdoor releases provided strong evidence that dry deposition is an important factor in the fate of a high-concentration Cl_2 plume under calm conditions [9]. Thus, deposition must be included in consequence assessment models to accurately predict the hazard area resulting from a large-scale Cl_2 release.

Previous laboratory [8] and field measurements [9] demonstrated that soil organic matter affected the Cl_2 deposition rate, so a single deposition velocity would be inadequate to universally predict Cl_2 deposition. An empirical relationship was derived to predict the deposition velocity from the fraction of soil organic matter and the Cl_2 exposure, but this was accomplished for soil blends with constant moisture content. The field measurements showed a positive correlation between the Cl_2 deposited and the moisture content; however, since there was also a positive correlation between organic matter and moisture content, the effect of moisture could not be resolved.

Water affects both the chemistry of Cl_2 deposition and gas-phase transport. Cl_2 reacts reversibly with water to produce HOCl and OCl^-, which oxidize organic molecules, providing an irreversible mechanism for Cl_2 deposition [10]. HCl is also formed, which can react with carbonate minerals, providing another

Table 1
Soil constituents (w/w) and density.

Constituent	Chemical formula	Compost (%)	Clay (%)	Sand (%)	Density[a] (g/cm³)
Organic content	N/A	10.2	2.3	0.45	0.9
Quartz	SiO_2	84.3	8.5	94.6	2.65
Clinochlore	$(Mg,Fe)_6(Al,Si)_4O_{10}(OH)_8$		36.9		2.65
Kaolinite	$Al_2Si_2O_5(OH)_4$	2.2			2.65
Muscovite	$KAl_3Si_3O_{10}(OH)_2$	3.4		2.5	2.83
Kyanite	Al_2SiO_5			0.4	3.59
Mn-Cordierite	$Mn_2(Al_4Si_5O_{18})$		7.3		2.66
Epidote	$Ca_2Al_2FeSi_3O_{12}OH$		12.0		3.44
Piemontite	$Ca_2AlMnSi_3O_{12}OH$		3.2		3.49
Albite	$NaAlSi_3O_8$		21.5		2.63
Anorthite	$CaAl_2Si_2O_8$				
Sanidine	$KAlSi_3O_8$		3.7		2.52
Phillipsite	$(Na,K,Ca)(Al,Si)_4O_8$		4.9		2.2
Calculated density[b] (g/cm³)		2.22	2.59	2.63	

[a] Densities were obtained from [14].
[b] Calculated densities determined from mass-weighted averages of constituent densities.

mechanism for irreversible deposition. Thus, regarding the chemistry of Cl_2 deposition, higher water content should act to accelerate the observed rate of reaction. However, partitioning into an immobile phase (in this case, water) is also known to slow transport through a porous bed of soil particles [11]. The effective diffusion coefficient for vapor transport is reduced by a tortuosity factor that is related to the void space and water content [12,13].

Therefore, the dependence of Cl_2 deposition on soil moisture content may not be a simple linear correlation. Here we examine Cl_2 deposition into soils with moisture contents from 0 to 0.2 (w/w) and with varying organic matter contents. We use the chloride ion (Cl^-) as a tracer for Cl_2 deposition to measure the depth of penetration of Cl_2 into the soil columns with the same nominal Cl_2 exposure. We expect to see evidence showing that water increases the effective reaction rate of Cl_2 but decreases the transport rate. These competing factors should yield a soil moisture of maximum Cl_2 deposition, below which Cl_2 deposition increases with increasing moisture and above which Cl_2 deposition decreases with increasing moisture.

2. Materials and methods

2.1. Synthetic soil characterization and preparation

Synthetic soil blends were made by mixing basalt clay (Welch Tennis Courts, Inc., Sun City, FL) with sand and compost (the latter two purchased from a local hardware store, Home Depot, Panama City, FL). Basalt clay and sand were used as received. Compost was sieved (#8 mesh, <2.56 mm particle size) to remove large particles. Mineral content and mass fraction of organic matter of starting materials were determined previously [8] and are listed in Table 1.

All soil constituents were dried in a 90 °C oven overnight to remove moisture. Dried starting materials were mixed and then water was added back into the mixtures at the indicated mass loadings (0–0.2). Soil types are named for the relative mass fractions of the three starting materials in this order: compost:clay:sand. Thus, soil type 4:1:1 contains (by mass) 4 parts compost and 1 part each of clay and sand. All samples were stored in sealed containers to minimize water loss prior to Cl_2 exposure. Synthetic soil blends were packed into nominally 5 cm × 10 cm (diameter × length) stainless steel columns. The columns were packed by adding a small amount of soil to the column, compacting the soil layer with a hand plunger, and repeating until the column was full. The total volume of a packed soil column was 163 cm³, and columns were weighed to obtain bulk soil density (ρ_{bulk}).

Column void fractions (ϕ) were determined from measured bulk soil densities (ρ_{bulk}) and estimated densities for soils with a void

fraction of zero (ρ_{solid}). ρ_{solid} was calculated from the measured abundances of the mineral and organic content of the starting materials using 0.9 g/cm³ as the density of the organic content and published mineral densities [14] (see Table 1). Mass-weighted averages of the starting material densities were used as ρ_{solid} for the soil mixtures. ϕ was then calculated using Eq. (1).

$$\phi = 1 - \frac{\rho_{bulk}}{\rho_{solid}} \tag{1}$$

Table 2 shows soil parameters ϕ, ρ_{bulk}, ρ_{solid}, organic content normalized to the soil column volume, and the maximum water volume fraction (θ_{max}).

2.2. Chlorine exposure

Six soil samples were exposed simultaneously in each experiment. The six samples were either different soil mixtures with the same moisture loading or the same soil mixture with different moisture loadings. For experiments with the same soil, one moisture loading was run in duplicate (i.e., 5 different water contents were used). The soil mixtures are denoted in the first column of Table 2 according to the notation described in Section 2.1. Six packed soil columns were exposed to vapor-phase Cl_2 (chemical purity grade, Airgas USA, LLC, Atlanta, GA) at ambient laboratory temperature (≈ 20 °C) in the deposition chamber described previously [8]. The assembled apparatus was purged with 0.5 L/min zero-grade compressed air (Airgas USA, LLC) for one hour prior to introduction of Cl_2. Cl_2 and air were introduced through separate ports approximately 10 cm from the base plate. The Cl_2 flow rate was initially set high to quickly reach a Cl_2 concentration ([Cl_2]) of $\approx 3 \times 10^4$ ppm in the chamber and then adjusted to maintain the [Cl_2]. [Cl_2] was measured in real time by a UV absorption cell described previously [8]. [Cl_2] was

Table 2
Soil Parameters.

Soil type	OC[a] (g/cm³)	ϕ[b]	ρ_{bulk} (g/cm³)	ρ_{solid} (g/cm³)	θ_{max}
1:0:0	0.11	0.51 ± 0.04	1.08 ± 0.09	2.22	0.27
4:1:1	0.088	0.48 ± 0.04	1.22 ± 0.10	2.33	0.30
1:1:1	0.061	0.43 ± 0.04	1.41 ± 0.11	2.47	0.35
1:1:4	0.035	0.43 ± 0.04	1.46 ± 0.11	2.55	0.36
1:4:1	0.053	0.36 ± 0.05	1.61 ± 0.13	2.53	0.31
0:1:0	0.041	0.32 ± 0.06	1.71 ± 0.16	2.59	0.34[c]

[a] Organic content.
[b] Void fraction (ϕ) calculated using Eq. (1).
[c] Soil mixture 0:1:0 with the maximum water content (θ_{max}) secreted water when packed.

Table 3
Description of variables.

Variable	Description	Units
C^*	C_g/C_{g0}	dimensionless
C_g	Gas-phase Cl_2 concentration	$mol/[m^3_{gas}]$
$C_{g0} = 2$	$C_g(z=0)$	$mol/[m^3_{gas}]$
$D = 10^{-5}$	Diffusion coefficient	m^2/s
$K = 0.01$	Solubility constant	$(mol/[m^3_{water}])/(mol/[m^3_{gas}])$
k	Rate constant	$[m^3_{soil\ column}]/mol/s$
$k' = 10–500$	kL^2/D	m^3/mol
$L = 0.1$	Soil column length	m
R	Soil constituent concentration	$mol/[m^3_{soil\ column}]$
R^*	R/R_0	dimensionless
$R_0 = 50–400$	$R(t=0)$	$mol/[m^3_{soil\ column}]$
t	Time	s
$T = 6$	tD/L^2	dimensionless
z	Depth	m
z^*	z/L	dimensionless
α	Air volume fraction	$[m^3_{gas}]/[m^3_{soil\ column}]$
θ	Water volume fraction	$[m^3_{water}]/[m^3_{soil\ column}]$
λ	$1 + \theta K/\alpha$	dimensionless
τ	Tortuosity factor	dimensionless
ϕ	Void fraction $(\theta + \alpha)$	$[m^3_{gas} + m^3_{water}]/[m^3_{soil\ column}]$

calculated using the Beer–Lambert law with a Cl_2 absorption cross section, σ_{330}, of 2.52×10^{-19} cm^2/molecule [15] and a path length of 10 cm. Cl_2 exposure time totaled 170 min, during which $[Cl_2]$ was above 10^4 ppm for 120 min. Exposures ($[Cl_2]t$) averaged $(3.9 \pm 0.9) \times 10^6$ ppm × min.

2.3. Sample analysis

Sample analysis was described previously [8]. Briefly, the soil columns were cored and vertically fractionated with a coring assembly consisting of a stainless steel tube with slits cut to accept a 2.5 cm radius spatula and a plunger to stop the corer when flush with the soil surface. The coring assembly had either coarse fractions (slits at 0.85, 1.69, 2.54, 5.08 and 7.62 cm from the soil surface) or fine fractions (slits at 0.48, 0.95, 1.43, 1.91, and 2.38 cm from the soil surface). Samples from each fraction (~1 g) were obtained and prepared for extraction (10 mL deionized water, 18 MΩ/cm) and subsequent analysis by ion chromatography [16] to measure Cl^- concentrations. Ion chromatography was performed in duplicate on an anion exchange column (4 × 250 mm IonPac® AS9-HC, Dionex®, Bannockburn, IL) with a mobile phase of 1.0 mL/min 9.0 mM Na_2CO_3 (pump model GP40, Dionex), and Cl^- was detected by a change in conductivity (detector model ED50, Dionex). A small flow of 25 mM H_2SO_4 was used to regenerate the suppressor (model ASRS®-ULTRA II 4 mm, Dionex). Standard solutions of NaCl (99%, Sigma–Aldrich) (0.0178–1.7836 mM) were analyzed to generate a calibration curve, and injections of a standard solution were made after every 10 samples.

2.4. Mathematical modeling

Deposition of Cl_2 into the soil columns was modeled using Fick's law of diffusion (Eq. (2)) and a simple rate law for Cl_2 reaction with reactive soil constituents (Eq. (3)), which are primarily organic matter. All variables are defined in Table 3. The quantity $(1 + \theta K/\alpha)$ in Eq. (2) is the retardation factor [11] (λ) and accounts for the slower transport of a chemical species through a porous material due to dissolution into the aqueous phase. The tortuosity factor (τ), defined in Eq. (4), is an empirical correction to gas-phase diffusion in a porous material [12,13].

$$\left(1 + \frac{\theta}{\alpha}K\right)\frac{\partial C_g}{\partial t} = \tau D \frac{\partial^2 C_g}{\partial z^2} - k\frac{\theta}{\alpha}KC_gR \tag{2}$$

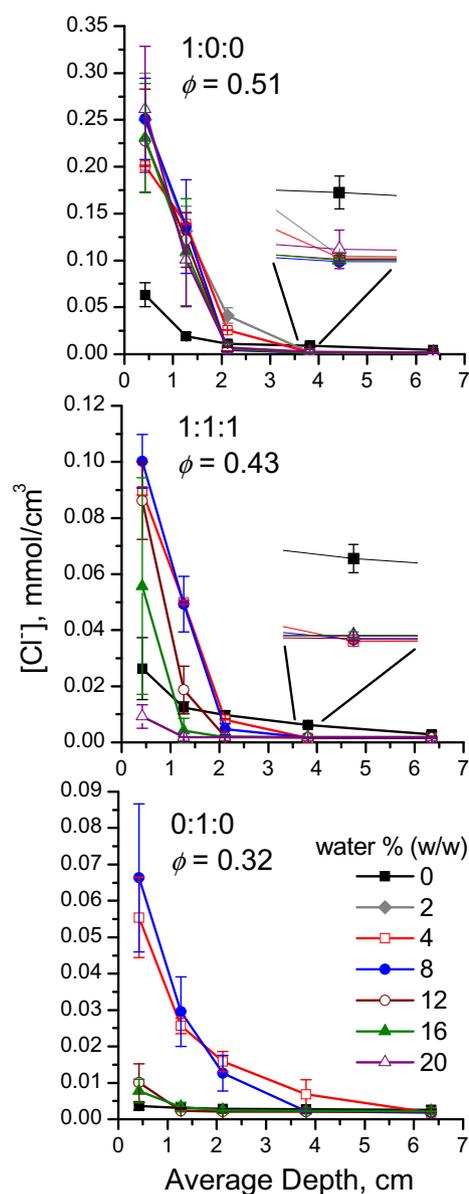$$\frac{\partial R}{\partial t} = -k\theta KC_gR \tag{3}$$

$$\tau = \frac{\alpha^{7/3}}{\phi^2} \tag{4}$$

It is helpful to use non-dimensionalized variables when solving transport equations, so the following variables were substituted into Eqs. (2) and (3): C^*, R^*, T, and z^*. In addition, k' was used, and substituting these variables into Eqs. (2) and (3) yield Eqs. (5) and (6).

$$\lambda \frac{\partial C^*}{\partial T} = \tau \frac{\partial^2 C^*}{\partial z^{*2}} - k'\frac{\theta}{\alpha}KC^*R_0R^* \tag{5}$$

$$\frac{\partial R^*}{\partial T} = -\theta k'KC_{g0}C^*R^* \tag{6}$$

Fig. 1. Deposition of Cl_2 (measured as $[Cl^-]$) as a function of depth using coarse vertical fractions. Soil types, ϕ, and water mass loadings are indicated. $[Cl^-]$ is normalized to the soil column volume, and error bars are the standard deviations of replicate measurements. Insets to the top two panels show a close-up of data at 3.8 cm deep to illustrate the higher $[Cl^-]$ detected in these dry soils.

Eqs. (5) and (6) were solved numerically using COMSOL Multiphysics®, a finite element solver. Boundary conditions were a constant Cl_2 concentration at the soil surface (C_{g0}) and zero Cl_2 flux at the base of the soil column ($z^* = 1$). Values or ranges for variables are disclosed in Tables 2 and 3; grid spacing (Δz^*) was 0.002. Values for D [17] and K [18] were obtained from the literature. L, C_{g0}, and T were set to values used in the experiments. R_0 was estimated from the experimental results, k' was estimated as described in Section 3.2, and ranges for α and θ were obtained as described in Section 2.1.

3. Results and discussion

3.1. Chamber measurements

Fig. 1 shows the effects of moisture content on three soil types analyzed with the coarse vertical fractions. All soils exhibit Cl^- for all moisture contents examined. Cl^- present in the dry samples suggests that there is some residual water in the soil columns, which is not surprising since it is unlikely that all the water is removed from the soil mixtures at 90 °C. Significantly more Cl^- is observed in all samples when water was added. For the 1:0:0 soil, just 2% (w/w) water loading yielded the same $[Cl^-]$ as that with 20% (w/w) water. This increased deposition of Cl_2 with added water is consistent with the chemical mechanism of dissolution followed by reaction.

While the 1:0:0 soil exhibits only minor changes in the deposition of Cl_2 for water contents from 2 to 20%, deposition in the other two soil mixtures is strongly dependent on the water loading. Both the 1:1:1 and 0:1:0 soils show increasing Cl_2 uptake to 8% water, but decreasing deposition at higher water loadings. This reduced deposition is evident in decreased $[Cl^-]$ in the top fraction and those deeper. For example, the 1:1:1 soil with 12% water content shows a slightly reduced $[Cl^-]$ in the top fraction relative to that with 8% water, but at 1.25 cm deep, there is a significant reduction in the 12% water sample. Further, the insets to the 1:0:0 and 1:1:1 soil mixture
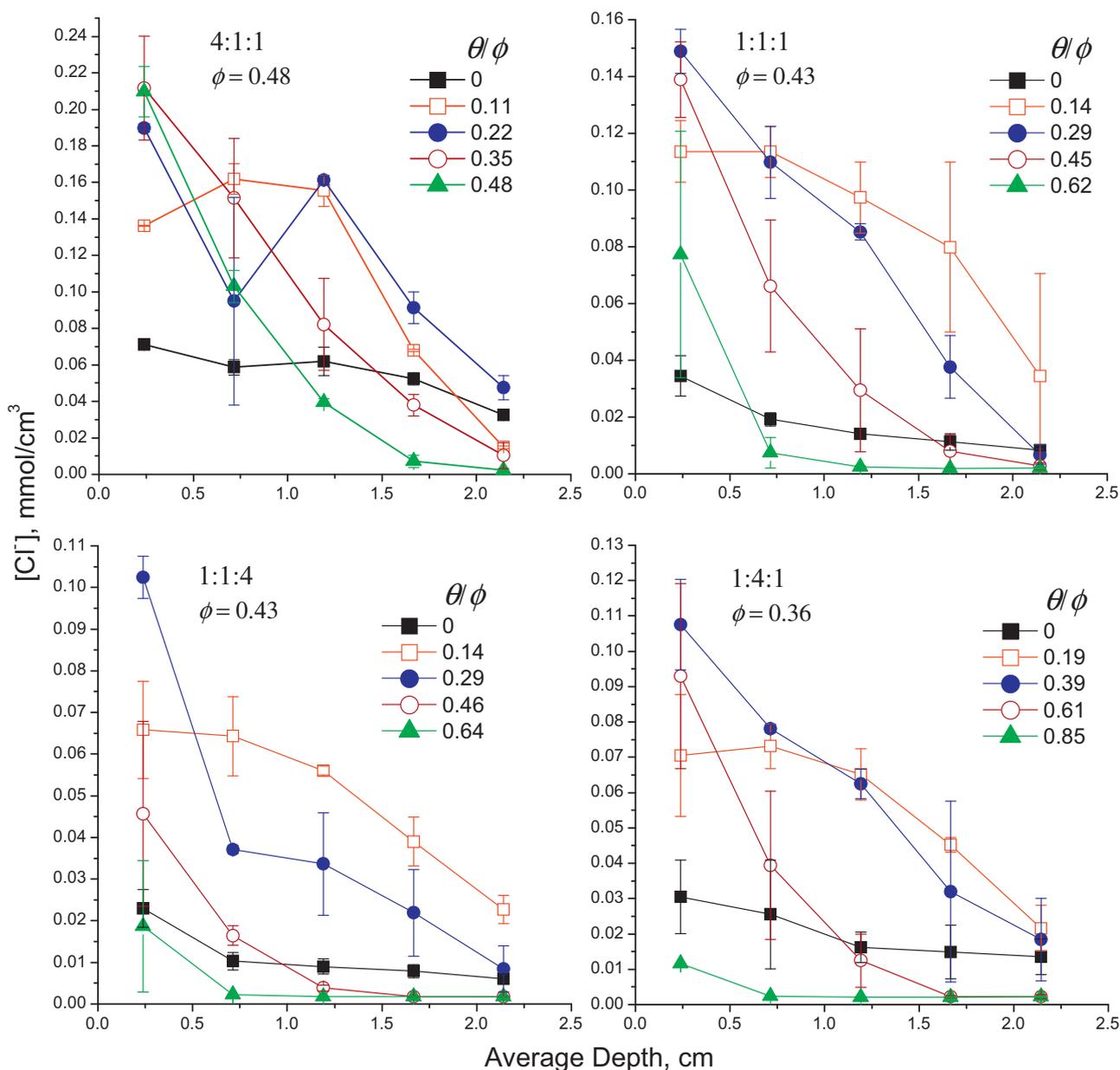

Fig. 2. Deposition of Cl_2 as a function of depth with finer vertical fractions. Soil types, ϕ, and θ/ϕ are indicated. Water mass loadings are 0, 4, 8, 12, and 16% for ■, □, ●, ○, and ▲, respectively. $[Cl^-]$ is normalized to the soil column volume, and error bars are the standard deviations of replicate measurements.

graphs in Fig. 1 show that at 3.8 cm deep the dry sample contains significantly more Cl^- than those with added water. These observations confirm that moisture does limit Cl_2 transport through soils in conditions similar to those encountered at a hazardous Cl_2 release.

In Fig. 1, very little Cl^- was detected at depths larger than ≈ 2 cm, so to provide a more detailed picture of Cl_2 deposition in soil, samples were vertically fractionated with finer resolution and additional mixtures were examined. Fig. 2 shows the results for the indicated soil mixtures to a depth of 2.2 cm. Soil type 4:1:1, similar to 1:0:0, shows no reduction in $[Cl^-]$ at the highest water content investigated (16%, $\theta/\phi = 0.48$); however, at the highest water content, Cl_2 does show lower deposition at the deeper fractions relative to those samples with less water.

While soil 4:1:1 exhibits similar Cl_2 deposition for moisture contents higher than the dry case, the other soil mixtures in Fig. 2 show significant effects of water on Cl_2 deposition. Soils 1:1:1, 1:1:4, and 1:4:1 show a maximum deposition in the top fraction at 8% (w/w) water. At 16% water, these soil mixtures exhibit very little penetration. From Fig. 1, Cl_2 deposits to a maximum depth of 0.85 cm for soil 1:1:1, and results from the more finely resolved fractions in Fig. 2 indicate that very little Cl_2 deposits deeper than 0.48 cm. Clearly, the higher water content affects Cl_2 transport. The legends in Fig. 2 show θ/ϕ, which is a measure of the fractional pore space filled with water and, therefore, unavailable for gas-phase transport. Soils 1:1:1 and 1:1:4 show very little deposition in fractions deeper than 0.48 for $\theta/\phi = 0.62$ and 0.64, whereas soil 1:4:1 shows significant deposition in deeper fractions for $\theta/\phi = 0.61$. However, at $\theta/\phi = 0.85$, Cl_2 deposition in the deeper fractions of soil 1:4:1 is zero.

It is clear that the void space in the soil column plays an important role in the overall deposition of Cl_2, and the amount of water affects α by filling the void space. However, the water may not only fill pore space, it could also affect the packing of the soil columns since samples were prepared with the prescribed amount of water already mixed in. To test whether better packing affects the observed depth penetration of Cl_2, six identical soil samples were prepared and three of them were dried in an oven at $60\,^{\circ}C$ for two days. All six samples were exposed to Cl_2 at the same time, so the only difference was the presence or absence of water. This experiment was repeated for soil 1:1:1 with 8% and 16% water loadings, and the results are shown in Fig. 3.

For the wet soils in Fig. 3, the depth profile of $[Cl^-]$ was similar to that observed in Fig. 2. Soil with 16% water loading showed very little Cl^- in the second fraction down, and soil with 8% water showed a nearly linear dependence of $[Cl^-]$ on depth. The dried soil columns exhibited only a small $[Cl^-]$ in the top fraction, consistent with the dry samples in Fig. 2. In addition, $[Cl^-]$ shows essentially no dependence on depth for the dried samples in Fig. 3. If water significantly affected the packing of the soil columns, the dried samples would show a similar depth profile of $[Cl^-]$ as the wet ones. Instead, Cl_2 transport is unhindered to a depth of 2.2 cm. Thus, the deeper relative penetration of Cl_2 in the dry samples of Figs. 1 and 2 is not due to an artifact of the column packing procedure. Further, the flat depth profile of the 18% water soil that was dried in Fig. 3 demonstrates that its packing does not hinder Cl_2 transport, so the sharp drop-off of $[Cl^-]$ at a depth of 0.7 cm for the highest water loading of soils 1:1:1, 1:1:4, and 1:4:1 in Fig. 2 is due primarily to water filling available void space.

3.2. Numerical modeling

There are several variables that affect Cl_2 deposition, C_{g0}, t, R_0, ϕ, and θ. In these experiments, C_{g0} and t were kept constant but the latter three parameters were varied. To corroborate the conclusion that water is decreasing the rate of transport of Cl_2
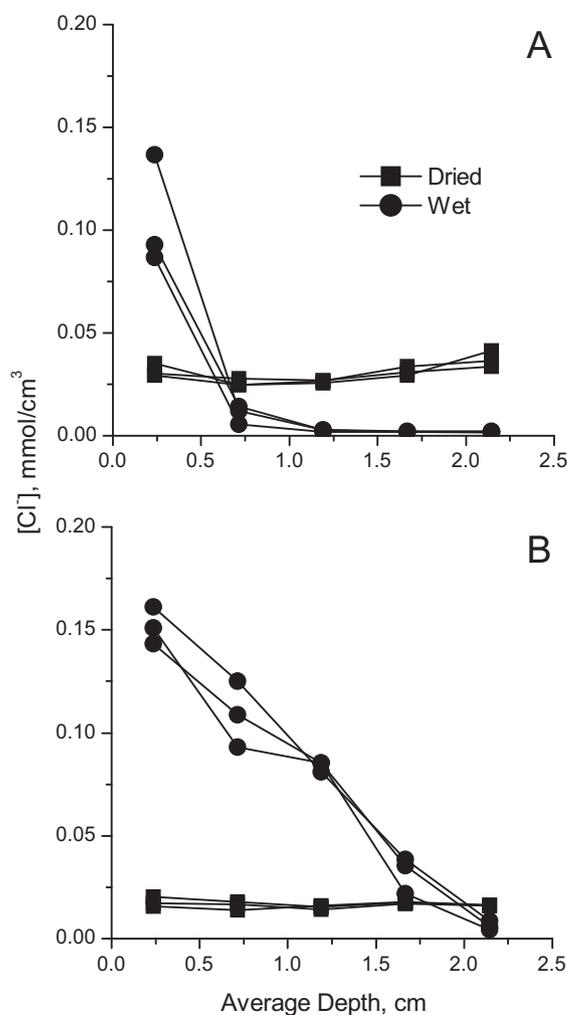

Fig. 3. Deposition of Cl_2 on soil 1:1:1 with (A) 16% (w/w) or (B) 8% (w/w) water content. All soil columns were packed while wet, then three columns in each experiment were dried at $60\,^{\circ}C$ for two days ($\blacksquare$) and the other three were covered to retain moisture until the experiment ($\bullet$). Columns in (A) and (B) were exposed to 3.4×10^6 and 3.8×10^6 ppm $\times$ min Cl_2, respectively.

through the soil column, Eqs. (5) and (6) were solved numerically using COMSOL. These equations use the non-dimensional variables T and z^*, C^*, and R^*, defined in Table 3. To generate model results that reasonably represent the conditions of these experiments, R_0 and k' must be known. Extrapolating the linear depth dependence of $[Cl^-]$ for soil 1:0:0 (which contained the highest amount of organic matter) in Fig. 1 to $z = 0$ yields approximately 0.28 mmol/cm^3, so an upper limit of 0.4 mmol/cm^3 (400 mol/m^3) was used for R_0. Soils 0:1:0 and 1:1:4 (both with low amounts of organic matter) exhibited maximum $[Cl^-]$ at about 0.1 mmol/cm^3, so a lower limit of 0.05 mmol/cm^3 (50 mol/m^3) was used for R_0. These lower and upper limits of R_0 adequately cover the experimental parameter space. The effective rate constant (k') was not known, thus k' was adjusted to find agreement with the experimental results.

Fig. 4 shows the results of the numerical solution to these partial differential equations, in which the effects of k', R_0, ϕ, and θ are shown. Note that the y axis is the amount of product formed normalized to the product formed at $T = \infty$, and the x axis is the normalized depth. While the focus of this work is on the effects of water on Cl_2 deposition, it is important to examine the effects of other variables in Eqs. (5) and (6) to garner a comprehensive understanding of the factors that affect deposition in soil
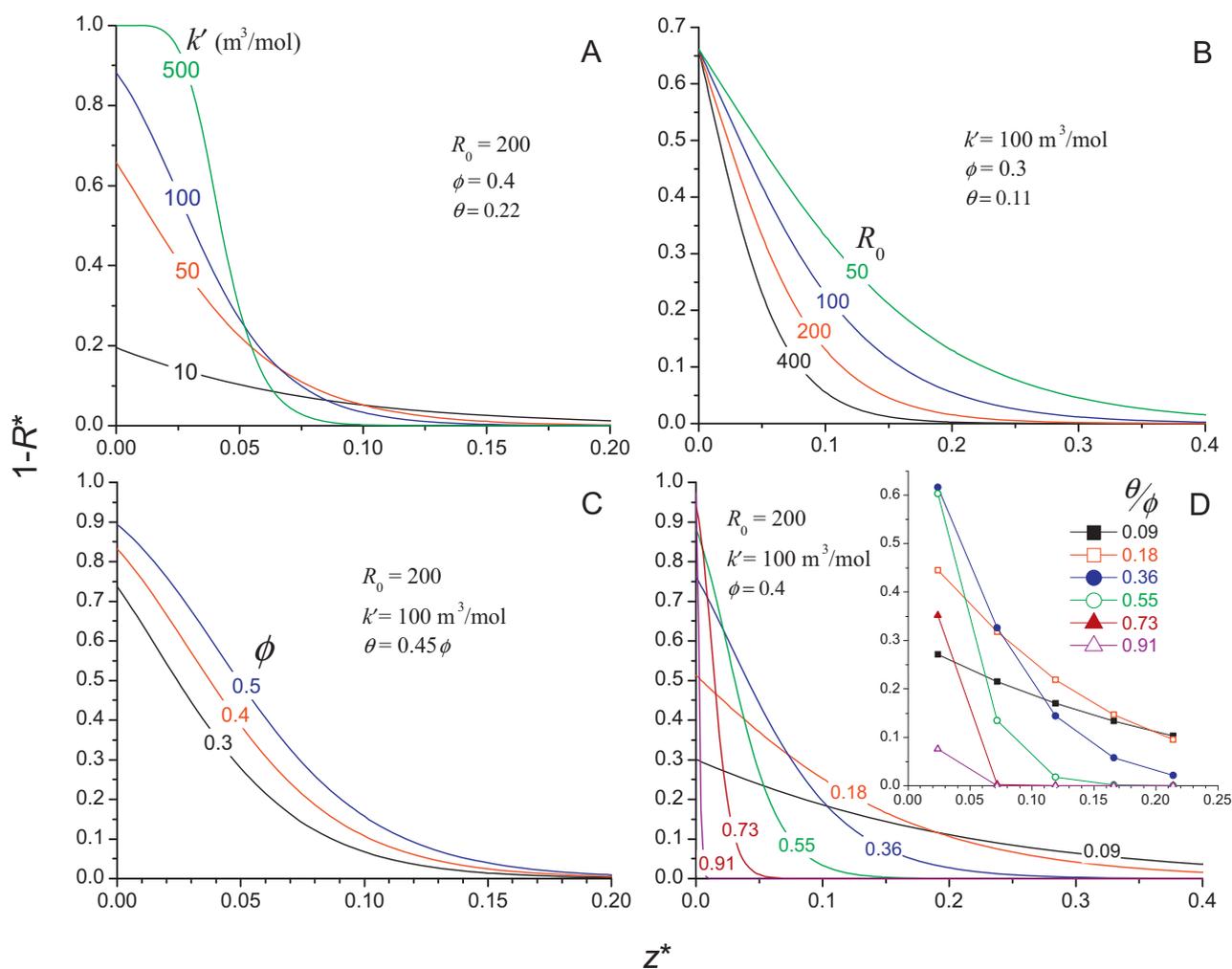
Fig. 4. Numerical modeling results for the variable quantities listed in each quadrant. (A), (B), (C), and (D) show the results for independently varying k', R_0, ϕ, and θ/ϕ, respectively. Inset to (D) shows the integrated numerical results to illustrate the effect of sampling with $\Delta z^* = 0.048$. Other parameters were $C_{g0} = 2$ mol/m^3, $T = 6$, and $K = 0.01$.

matrices. In panel A, faster k' increases the amount of product near the soil surface ($z^* < 0.05$), but decreases the amount of product at larger depths. The effective aqueous-phase rate constant (k') was unknown, but a value of 100 m^3/mol approximates the depth dependence of the product concentration observed in the data of Fig. 2 with similar θ/ϕ. Thus, $k' = 100$ m^3/mol was used for the numerical results in the other panels of Fig. 4. Panel B shows that higher R_0 does not affect the relative amount of product at the surface ($z = 0$), but it does reduce the relative penetration of Cl$_2$. Panel C shows the effect of void space (ϕ), and a larger amount of void space yields more product and deeper penetration. Note that in Panel C that θ/ϕ is kept constant for the three values of ϕ.

Finally, Fig. 4D shows the effects of water on the deposition of Cl$_2$. Increasing the water fraction decreases Cl$_2$ depth of penetration and increases the product concentration at the surface ($z = 0$). As a more direct comparison with the experimental results, the inset to Fig. 4D shows the numerical modeling results integrated over the depth fractions used in the experimental analysis. The same trend is observed in the numerical results as those in Figs. 1 and 2. High water content attenuates the transport of Cl$_2$ into deeper soil fractions, and the top fraction exhibits significantly less product at high water contents. These results corroborate the conclusion from the experimental results.

As further comparison between numerical modeling and experimental results, Fig. 5 shows results from the top 0.48-cm fraction for each. Experimental results (Fig. 5B) show peaks in the product yield at $\theta/\phi = 0.3$–0.4, and the modeling results (Fig. 5A) show peaks in the product yield at progressively higher θ/ϕ for higher R_0. The θ/ϕ range for the modeling results (0.4–0.55) is near those of the experiments. However, the experimental results show no apparent trend of the θ/ϕ value for the product peak with the organic concentration (note organic content in Table 2). This may indicate that other processes or factors are not adequately accounted for in Eqs. (5) and (6). Nevertheless, the similar trends observed in the modeling and experimental results support the conclusion that water restricts transport of Cl$_2$ into the soil column.

As mentioned in Section 1, water's restriction of vapor transport through a porous soil matrix is established in the literature. However, much of the environmental literature is concerned with longer time scales and lower concentrations than that relevant to the transport and evolution of hazardous chemical plumes. The experiments and numerical solutions here show that in the case of Cl$_2$, the same mechanism is operable for deposition of Cl$_2$ into a soil matrix for conditions that are relevant for hazard prediction and analysis (high [Cl$_2$] for a couple of hours). However, water in these experiments was stationary (i.e., there was no advective transport of water). For conditions of water flow (e.g., rainwater
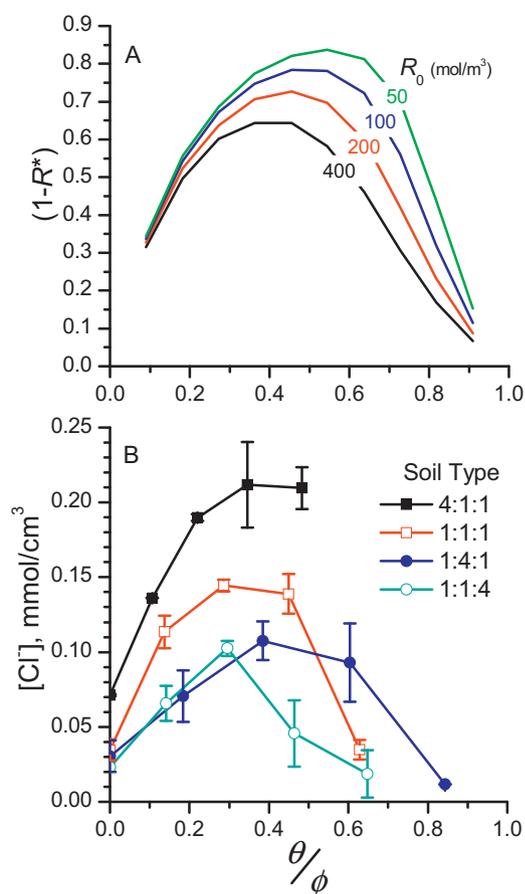
Fig. 5. Comparison of top fraction results ($\Delta z = 0.48$ cm) from (A) numerical modeling and (B) experimental results. Numerical solutions were obtained using $T = 6$, $\phi = 0.5$, and the indicated R_0s (mol/m^3). Experimental results are those from Fig. 2 plotted against θ/ϕ.

seeping through the soil), the added transport term would change the results.

4. Conclusions

Cl$_2$ deposition was measured on synthetic soil blends with the aim of elucidating the role of soil moisture content on the rate of Cl$_2$ removal. Experimental results demonstrated that water increased the rate of reaction but it decreased the vapor transport through the soil column. The maximum Cl$_2$ deposited corresponded to conditions for which the water volume fraction was approximately half of the total void space in the soil matrix. Numerical solutions to transport and reaction equations that describe the problem confirmed

the conclusions. On a final note, we remind the reader that these results represent conditions for which condensed phase water is stationary. For conditions where water is moving, the results will be different.

References

[1] S. Hanna, R. Britter, E. Argenta, J. Chang, The Jack Rabbit chlorine release experiments: implications of dense gas removal from a depression and downwind concentrations, J. Hazard. Mater. 213–214 (2012) 406–412.

[2] S. Hanna, S. Dharmavaram, J. Zhang, I. Sykes, H. Witlox, S. Khajehnajafi, K. Koslan, Comparison of six widely-used dense gas dispersion models for three recent chlorine railcar accidents, Process Saf. Prog. 27 (2008) 248–259.

[3] R.L. Buckley, C.H. Hunter, D.W. Werth, M.T. Whiteside, K.-F. Chen, C.A. Mazzola, A case study of chlorine transport and fate following a large accidental release, Atmos. Environ. 62 (2012) 184–198.

[4] M.B. Dillon, The role of deposition in limiting the hazard extent of dense-gas plumes, J. Hazard. Mater. 164 (2009) 1293–1303.

[5] M. Mochida, J. Hirokawa, Y. Kajii, H. Akimoto, Heterogeneous reactions of Cl$_2$ with sea salts at ambient temperature: Implications for halogen exchange in the atmosphere, Geophys. Res. Lett. 25 (1998) 3927–3930.

[6] J.H. Hu, Q. Shi, P. Davidovits, D.R. Worsnop, M.S. Zahniser, C.E. Kolb, Reactive uptake of Cl$_2$(g) and Br$_2$(g) by aqueous surfaces as a Function of Br$^-$ and I$^-$ ion concentration: the effect of chemical reaction at the interface, J. Phys. Chem. 99 (1995) 8768–8776.

[7] A.C. Hill, Vegetation, A sink for atmospheric pollutants, J. Air Pollut. Control. Assoc. 21 (1971) 341–346.

[8] J. Hearn, J. Eichler, C. Hare, M. Henley, Cl$_2$ deposition on soil matrices, J. Hazard. Mater. 237–238 (2012) 307–314.

[9] J.D. Hearn, R. Weber, R. Nichols, M.V. Henley, S. Fox, Deposition of Cl$_2$ on soils during outdoor releases, J. Hazard. Mater. 252–253 (2013) 107–114.

[10] G.C. White, Handbook of Chlorination, Van Nostrand Reinhold, New York, 1972.

[11] C. Zheng, G. Bennet, Applied Contaminant Transport Modeling: Theory and Practice, Van Nostrand Reinhold, New York, 1995.

[12] A.L. Baehr, Selective transport of hydrocarbons in the unsaturated zone due to aqueous and vapor phase partitioning, Water Resour. Res. 23 (1987) 1926–1938.

[13] C.A. Shoemaker, T.B. Culver, L.W. Lion, M.G. Peterson, Analytical models of the impact of two-phase sorption on subsurface transport of volatile chemicals, Water Resour. Res. 26 (1990) 745–758.

[14] D.R. Lide, CRC Handbook of Chemistry and Physics, 76 ed., CRC Press, Inc., Boca Raton, FL, 1995.

[15] S. Hubinger, J.B. Nee, Absorption spectra of Cl$_2$, Br$_2$ and BrCl between 190 nm and 600 nm, J. Photochem. Photobiol. A: Chem. 86 (1995) 1–7.

[16] Determination of Inorganic Anions by Ion Chromatography, EPA Method 9056A, 2007, http://www.epa.gov/wastes/hazard/testmethods/sw846/pdfs/9056a.pdf

[17] C.L. Yaws, Yaws Handbook of Properties of the Chemical Elements, Knovel, Norwich, NY, 2011, www.knovel.com. Electronic ISBN: 978-1-61344-399-6.

[18] M. Alkan, M. Oktay, M.M. Kocakerim, M. Çopur, Solubility of chlorine in aqueous hydrochloric acid solutions, J. Hazard. Mater. 119 (2005) 13–18.